Molecular Therapy
Nucleic Acids
Original Article

Regulatory Role of the MicroRNA-29b-IL-6 Signaling in the Formation of Vascular Mimicry

Jian-Hong Fang,[1,3] Zhi-Yuan Zheng,[1,3] Jin-Yu Liu,[1] Chen Xie,[2] Zi-Jun Zhang,[1] and Shi-Mei Zhuang[1,2]

[1]Key Laboratory of Gene Engineering of the Ministry of Education, State Key Laboratory of Biocontrol, Collaborative Innovation Center for Cancer Medicine, School of Life Sciences, Sun Yat-sen University, Guangzhou 510275, China; [2]Key Laboratory of Liver Disease of Guangdong Province, The Third Affiliated Hospital, Sun Yat-sen University, Guangzhou 510630, China

Vascular mimicry (VM) is a critical complement for microcirculation and is implicated in tumor progression. We showed that IL-6 derived from tumor cells and stroma cells promoted tumor cells to form a VM structure, whereas blocking the IL-6 signaling by RNA interference, IL-6-neutralizing antibody, or STAT3 inhibitor suppressed the VM formation of tumor cells. Mechanism investigations revealed that IL-6 stimulated VM formation by activating STAT3, in turn upregulating VE-cadherin expression and MMP2 activity. Further analyses identified a positive association between the activation of IL-6-STAT3 signaling and the formation of the VM structure in human HCC tissues. However, miR-29b repressed the expression of STAT3 and MMP2 by directly binding to the 3′ UTRs of their mRNAs. Consistently, both gain- and loss-of-function analyses showed that miR-29b suppressed tumor cells to form tube structures in vitro. The in vivo studies further disclosed that intratumoral injection of the miR-29b-expressing viruses significantly inhibited the IL-6-promoted VM formation in mouse xenografts, and downregulation of miR-29b was correlated with the presence of VM in human HCC tissues. This study elucidates a miR-29b-IL-6 signaling cascade and its role in VM formation, which provide potential targets for cancer therapy.

INTRODUCTION

Interleukin-6 (IL-6), one of the key inflammatory cytokines, can be generated by tumor cells or tumor stromal cells, such as tumor-associated macrophages (TAMs) or fibroblasts.[1–5] High IL-6 activity may promote tumor development by suppressing cell apoptosis and promoting tumor proliferation, angiogenesis, and metastasis.[2,3,6,7] IL-6 signals through a receptor composed of two subunits: IL-6 receptor (IL-6R) that possesses ligand specificity and glycoprotein 130 that is common for interleukin family members.[1,8] Binding of IL-6 to its receptor activates JAK kinases and in turn stimulates STAT transcription factors, particularly STAT3.[1,2,8] It has been disclosed that the IL-6-dependent STAT3 activation is a prevalent event in tumor cells and is associated with excessive growth, invasion, and angiogenesis of cancers.[1,7,8]

Vascular mimicry (VM) is a recently identified vascular channel-like structure that consists of tumor cells, but not endothelial cells, and displays positive staining for periodic acid-Schiff (PAS) and negative staining for CD34. VM provides adequate blood supply for tumors[9,10] and is implicated in tumor growth and metastases, correlated with short survival of malignant tumors.[11–15] It is proposed that VM may complement the endothelial cell-dependent angiogenesis, especially at the early stage of tumor development.[16–18] VM is independent of endothelial cells, which may partly explain why anti-cancer drugs targeting angiogenesis have not achieved the expected success,[18–20] Therefore, identifying molecules that suppress VM formation may provide targets for cancer therapy. The VE-cadherin (VE-Cad) and its downstream EphA2-PI3K/Akt-MMP2 signaling cascade have been shown to be critical for VM formation.[9,10,13] Although IL-6 signaling is frequently activated in cancers, such as hepatocellular carcinoma (HCC),[2,7] its effect in VM formation has not been reported yet.

We previously found that microRNA-29b (miR-29b) was frequently downregulated in HCC and associated with poor survival of patients; miR-29b promoted cell apoptosis by inhibiting Bcl-2 and Mcl-1 expression and inhibited tumor angiogenesis and metastasis via suppressing MMP2 expression.[21,22] A study from another group revealed that miR-29b could also inhibit tumor proliferation by targeting CDK6.[23] However, the regulatory role of miR-29b in VM formation and IL-6 signaling remains unknown.

In an attempt to identify the molecules that regulated VM formation, we disclosed that IL-6 derived from tumor cells and stromal cells could promote VM formation. Mechanism investigations revealed that IL-6 upregulated VE-Cad expression and MMP2 activity by activating STAT3, which consequently promoted VM formation. However, miR-29b could abolish the IL-6-promoted VM formation by directly inhibiting STAT3 and MMP2 expression. These findings explore a miRNA-29b-IL-6 signaling pathway and its regulatory role in VM formation.

RESULTS

IL-6-STAT3 Signaling Promotes the Tube Formation of Tumor Cells

To evaluate the effect of IL-6 signaling on VM formation, we first employed a well-established three-dimensional tube formation assay to

Received 21 May 2017; accepted 13 June 2017;
http://dx.doi.org/10.1016/j.omtn.2017.06.009.

[3]These authors contributed equally to this work.

Correspondence: Shi-Mei Zhuang, School of Life Sciences, Sun Yat-sen University, Xin Gang Xi Road 135#, Guangzhou 510275, China.
E-mail: zhuangshimei@163.com

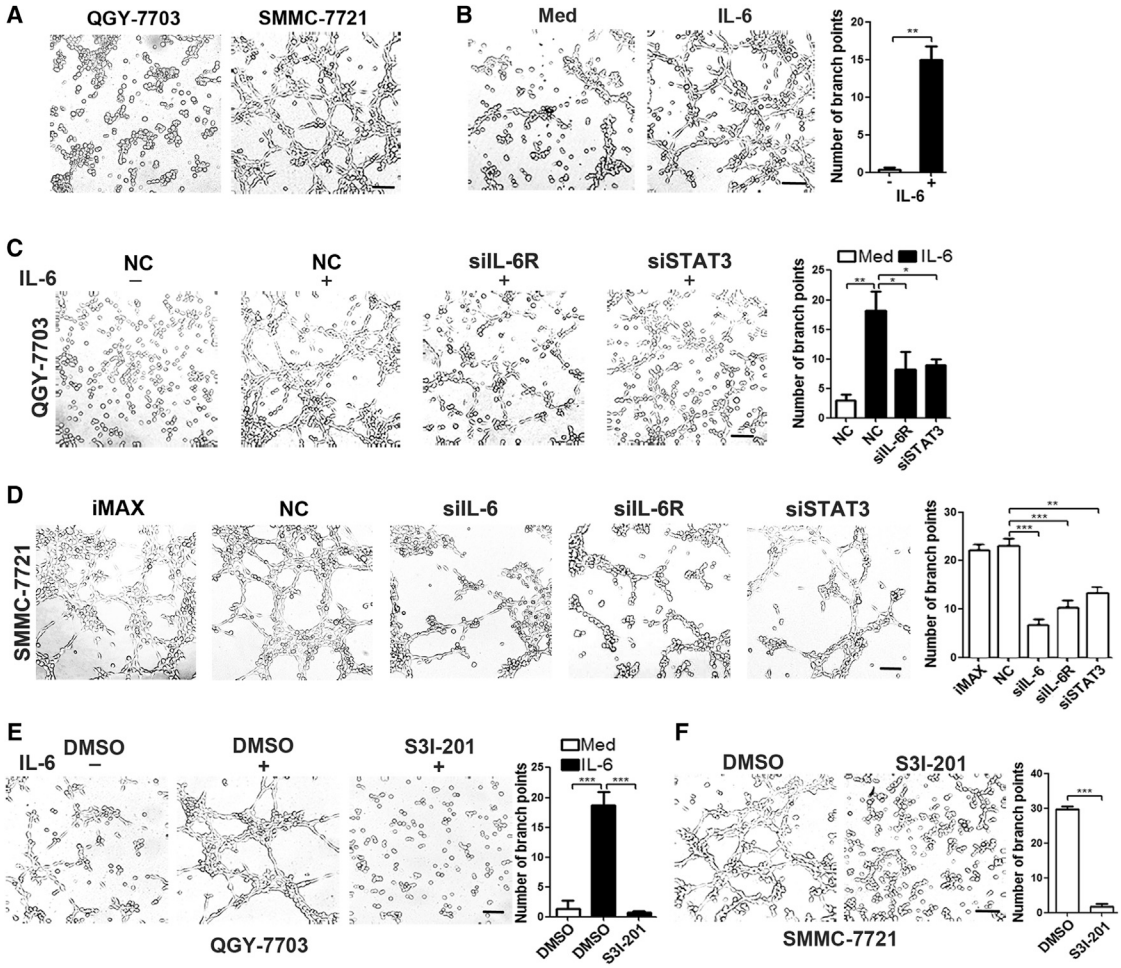

Figure 1. IL-6-STAT3 Signaling Promotes the Tube Formation of Tumor Cells In Vitro

(A) QGY-7703 and SMMC-7721 cells displayed different capacities to form capillary-like tube structure. (B) IL-6 promoted capillary-like tube formation. QGY-7703 cells were stimulated with IL-6 for 24 hr, followed by tube formation assay. (C) The IL-6-promoted tube formation was inhibited by silencing IL-6R or STAT3. QGY-7703 cells were transfected with the indicated siRNA duplex for 24 hr and then cultured without (–) or with (+) IL-6 for another 24 hr, followed by tube formation assay. Data are from four independent experiments. (D) The tube formation of SMMC-7721 cells was inhibited by knocking down the expression of IL-6, IL-6R, or STAT3. Cells were transfected with the indicated siRNA duplex for 36 hr, followed by tube formation assay. (E) S3I-201 abolished the IL-6-promoted tube formation of QGY-7703 cells. Cells were cultured without or with S3I-201 or IL-6 for 24 hr, followed by tube formation assay. (F) S3I-201 inhibited the spontaneous tube formation of SMMC-7721 cells. Cells were stimulated with S3I-201 for 24 hr, followed by tube formation assay. For (B)–(F), the representative images of tube formation and the number of branch points of tubes are presented. "–" or Med indicates the cells that were cultured in DMEM with 5% FBS. IL-6 indicates the cells that were cultured in DMEM containing 5% FBS and IL-6. iMAX indicates the cells that were treated with Lipofectamine RNAiMAX without any RNA duplex. NC indicates the cells that were transfected with the negative control RNA duplex. DMSO indicates vehicle control for S3I-201. Scale bar, 50 μm. Error bar, SEM. *$p < 0.05$; **$p < 0.01$; ***$p < 0.001$. See also Figure S1.

examine the ability of different tumor cells to form VM in vitro. Two tumor cell lines (QGY-7703 and SMMC-7721), which displayed distinct activity of VM formation, were chosen for further investigation. Compared with QGY-7703, SMMC-7721 cells had a stronger ability to form a capillary-like tube structure (Figure 1A). The levels of IL-6 and IL-6R in SMMC-7721 cells were also higher than in QGY-7703 (Figure S1). Furthermore, IL-6 promoted QGY-7703 cells to form capillary-like tubes (Figure 1B), whereas knockdown of IL-6R or STAT3 in QGY-7703 cells abolished the IL-6-promoted tube formation (Figure 1C). Consistently, tube formation of SMMC-7721 cells was also dramatically inhibited when IL-6, IL-6R, or STAT3 was silenced (Figure 1D). Moreover, treatment with S3I-201, a specific inhibitor of STAT3, suppressed the IL-6-promoted tube formation of QGY-7703 cells (Figure 1E) and the spontaneous tube formation of SMMC-7721 cells (Figure 1F). These results indicate that activation of IL-6 signaling may promote VM formation of tumor cells.

IL-6 is not only secreted by tumor cells but also produced by stromal cells, such as cancer-associated fibroblasts (CAFs) and TAMs.[1,4,5] As

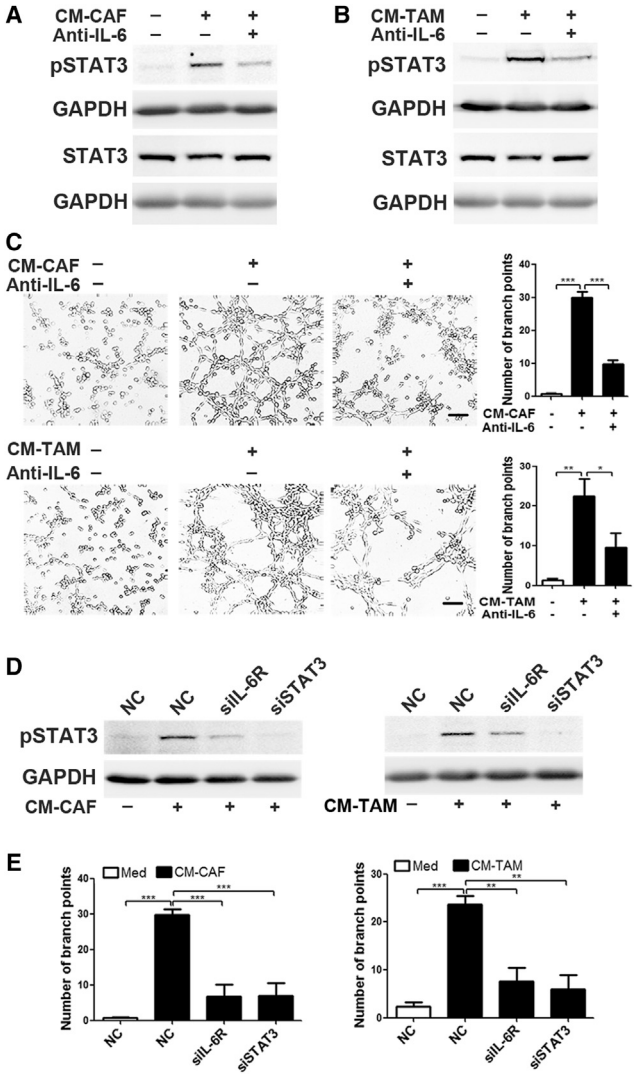

Figure 2. Tumor Stromal Cells Promote VM Formation In Vitro by Activating IL-6 Signaling

(A and B) Blocking IL-6 abrogated CM-CAF- and CM-TAM-induced STAT3 phosphorylation. QGY-7703 cells were cultured in CM-CAF (A) or CM-TAM (B) without (–) or with (+) treatment of IL-6-neutralizing antibody (anti-IL-6) for 1 hr before immunoblotting. (C) Blocking IL-6 inhibited the CM-CAF- and CM-TAM-promoted tube formation in vitro. QGY-7703 cells were cultured in CM-CAF (upper) or CM-TAM (lower) without (–) or with (+) anti-IL-6 for 36 hr before tube formation assay. The representative images and the number of branch points of tubes are presented. Scale bar, 50 μm. (D) Silencing IL-6R or STAT3 attenuated CM-CAF- or CM-TAM-induced STAT3 phosphorylation. QGY-7703 cells were transfected with the indicated RNA duplex for 36 hr and then cultured without (–) or with (+) CM-CAF or CM-TAM for 1 hr, followed by immunoblotting. (E) Silencing IL-6R or STAT3 inhibited the CM-CAF- or CM-TAM-promoted tube formation in vitro. QGY-7703 cells were transfected with the indicated RNA duplex for 24 hr and then cultured without (Med) or with CM-CAF or CM-TAM for another 24 hr, followed by tube formation assay. For treatment of CM-TAM (lower), data are from four independent experiments. For (A)–(E), "–" or Med indicates the cells that were grown in DMEM with 5% FBS. CM-CAF or CM-TAM indicates the cells that were grown in a mixture of equal volume of CM-CAF/CM-TAM and serum-free DMEM. GAPDH indicates internal control. Error bar, SEM. *p < 0.05; **p < 0.01; ***p < 0.001. See also Figure S2.

expected, the level of IL-6 in the conditioned medium (CM) derived from both CAFs (CM-CAF) and TAMs (CM-TAM) was much higher than that in the CM from non-activated normal fibroblasts (CM-NF) and macrophages (Figures S2A and S2B). Consistently, compared with CM-NF or CM from macrophages, CM-CAF and CM-TAM had a much stronger ability to increase the level of Tyr705-phosphorylated STAT3 (pSTAT3), a marker indicating the activation of IL-6-STAT3 signaling[8] (Figures S2C and S2D), and to promote the tube formation of QGY-7703 cells (Figures S2E and S2F). The CM-CAF- and CM-TAM-promoted STAT3 phosphorylation and tube formation were significantly attenuated when IL-6 in CM-CAF and CM-TAM was neutralized by antibody (Figures 2A–2C) or when IL-6R or STAT3 expression was silenced in QGY-7703 cells (Figures 2D and 2E).

Altogether, IL-6, which was secreted by tumor cells or stromal cells, may promote tube formation of tumor cells in vitro.

IL-6-STAT3 Signaling Upregulates VE-Cad Expression and MMP2 Activity

We then explored the mechanisms by which IL-6 promoted VM formation. Studies indicate that changes of vessel-associated molecules and remodeling of the extracellular matrix (ECM) play important roles in VM formation.[9,10,12–14] Among these genes, VE-Cad, MMP2, and MMP9 were well-defined to be critical for VM formation. Because the level of MMP9 in both SMMC-7721 and QGY-7703 cells was extremely low (data not shown), the roles of VE-Cad and MMP2 in the IL-6-promoted VM formation were further investigated. As shown, IL-6 treatment not only increased the mRNA levels of VE-Cad and MMP2 (Figure S3) but also enhanced the VE-Cad protein level and MMP2 activity in QGY-7703 cells (Figures 3A and 3B). Furthermore, blocking IL-6 signaling, by silencing IL-6R or STAT3 or treatment with S3I-201, reduced VE-Cad expression and MMP2 activity in IL-6-stimulated QGY-7703 cells (Figures 3C and 3D) and in SMMC-7721 cells (Figures S4A and S4B). Consistently, knockdown of VE-Cad or MMP2 in QGY-7703 cells abolished the IL-6-promoted tube formation (Figures 3E and 3F).

Further analyses in clinical samples showed that 34.9% (22/63) of human HCC tissues had VM structures, which were identified by the vascular channels that contained red blood cells and were lined by tumor cells, but not endothelial cells (PAS^+CD34^-) (Figure 3G, left). The cases with VM structure in the HCC section were designated VM^+, and those without VM in a whole HCC section were designated VM^-. The nuclear staining of Tyr705-pSTAT3 (Figure 3G, middle) was detected in 91% VM^+ cases (20/22), but only in 39.0% (16/41) VM^- ones, and the fraction of cells with nuclear pSTAT3 staining was significantly higher in VM^+ specimens compared with VM^- tissues (Figure 3G, right), suggesting a positive association between the activation of IL-6-STAT3 signaling and the formation of the VM structure in HCC tissues.

Collectively, these results imply that IL-6 may enhance VE-Cad expression and MMP2 activity by activating STAT3, which consequently results in VM formation.

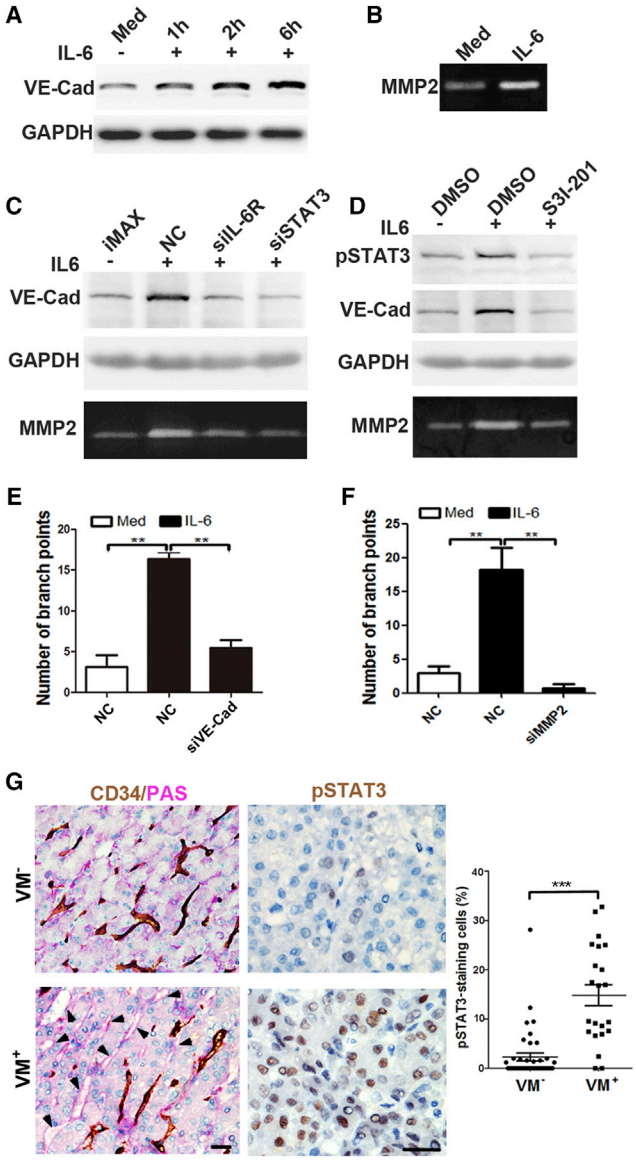

Figure 3. IL-6-STAT3 Signaling Promotes VM Formation by Upregulating VE-Cad and MMP2

(A) IL-6 treatment increased the level of VE-Cad protein. QGY-7703 cells were cultured in serum-free DMEM for 24 hr, followed by incubation with the refreshed serum-free medium without (Med) or with IL-6 for the indicated time before immunoblotting. (B) IL-6 treatment enhanced the activity of MMP2. QGY-7703 cells were cultured in serum-free DMEM without (Med) or with IL-6 for 24 hr; the conditioned medium was then applied to gelatin zymography analysis. (C) Knockdown of IL-6R or STAT3 attenuated IL-6-stimulated VE-Cad expression and MMP2 activity. After transfection with the indicated RNA duplex, QGY-7703 cells were either stimulated with IL-6 (in DMEM with 10% FBS) for 24 hr before immunoblotting (upper and middle) or stimulated with IL-6 (in serum-free DMEM) for 24 hr before gelatin zymography analysis for MMP2 activity (lower). iMAX indicates the cells that were transfected with Lipofectamine RNAiMAX without any RNA duplex. NC indicates the cells that were transfected with the negative control RNA duplex. (D) S3I-201 treatment reduced IL-6-stimulated VE-Cad expression and MMP2 activity. For immunoblotting, QGY-7703 cells were cultured in serum-free DMEM for 24 hr, followed by incubation with serum-free DMEM without or with S3I-201 or IL-6 for 2 hr. For gelatin zymography analysis, cells were cultured in serum-free DMEM without or with S3I-201 or IL-6 for 24 hr. DMSO was used as a vehicle control for S3I-201. (E and F) Knockdown of VE-Cad or MMP2 abolished the IL-6-promoted tube formation. QGY-7703 cells were transfected with NC, siVE-Cad (E), or siMMP2 (F) for 24 hr and then cultured in 5% FBS-containing DMEM without (Med) or with IL-6 for another 24 hr before tube formation assay. The number of the branch points of tubes is presented. **$p < 0.01$. For (A), (C), and (D), GAPDH was used as an internal control for immunoblotting. (G) The fraction of pSTAT3-staining cells was higher in human VM^+ HCC tissues. Left: double-staining for human CD34 and PAS. Middle: staining for human pSTAT3. Right: the fractions of pSTAT3-staining cells (as a percentage) in VM^- tissues (n = 41) and VM^+ tissues (n = 22). VM structures were identified by the vascular channels that contained red blood cells and were lined by tumor cells, but not endothelial cells (PAS^+CD34^-, indicated by arrowheads). The endothelial vessels were stained brown by antibody against CD34. Scale bar, 50 μm. Error bar, SEM. ***$p < 0.001$. See also Figures S3 and S4.

miR-29b Abolishes IL-6-Promoted VM Formation by Inhibiting STAT3 and MMP2 Expression

The preceding data disclosed the importance of IL-6 signaling on VM formation. Thus, targeting the IL-6 pathway may be an efficient way to inhibit VM formation and subsequent tumor growth. MicroRNA (miRNA) is an attracting molecule, because it may regulate cellular activity by targeting multiple genes.[24,25] In a previous study, we observed that miR-29b directly suppressed MMP2 expression by binding to its 3′ UTR.[21] Here, we demonstrated that miR-29b also significantly inhibited the activity of firefly luciferase that carried wild-type, but not mutant 3′ UTR of MMP2 in QGY-7703 and SMMC-7721 cells (Figure 4A; Figure S5A). Moreover, overexpression of miR-29 reduced the MMP2 activity in these cell lines (Figure 4B; Figure S5B). Because QGY-7703 cells displayed a higher miR-29b level than that of SMMC-7721 cells (data no shown), we analyzed the effects of antagonizing endogenous miR-29b in QGY-7703 cells. Consistently, inhibition of miR-29b enhanced MMP2 activity (Figure 4C).

STAT3 was also predicted as a target of miR-29b by TargetScan (Human 6.2) and MiRanda (August 2010 release). A dual-luciferase reporter assay showed that co-transfection of miR-29b significantly inhibited the activity of luciferase with wild-type 3′ UTR of STAT3, yet this effect was abrogated when the predicted miR-29b-binding site in the 3′ UTR was mutated (Figure 4D; Figure S5C). Moreover, introduction of miR-29b reduced the levels of STAT3 and its phosphorylated form (Figure 4E; Figures S5D and S5E), whereas antagonism of endogenous miR-29b upregulated STAT3 protein (Figure 4F). Consistently, human HCC tissues with lower miR-29b expression displayed higher levels of pSTAT3 (Figure 4G; Figure S6) and MMP2.[21] These results suggest that miR-29b may function as a repressor of STAT3 and MMP2.

The role of miR-29b on VM formation was then examined. Restoration of miR-29b expression in tumor cells significantly suppressed the IL-6-promoted tube formation of QGY-7703 (Figure 5A) and the spontaneous tube formation of SMMC-7721 cells (Figure 5B). In contrast, antagonism of endogenous miR-29b in QGY-7703 cells

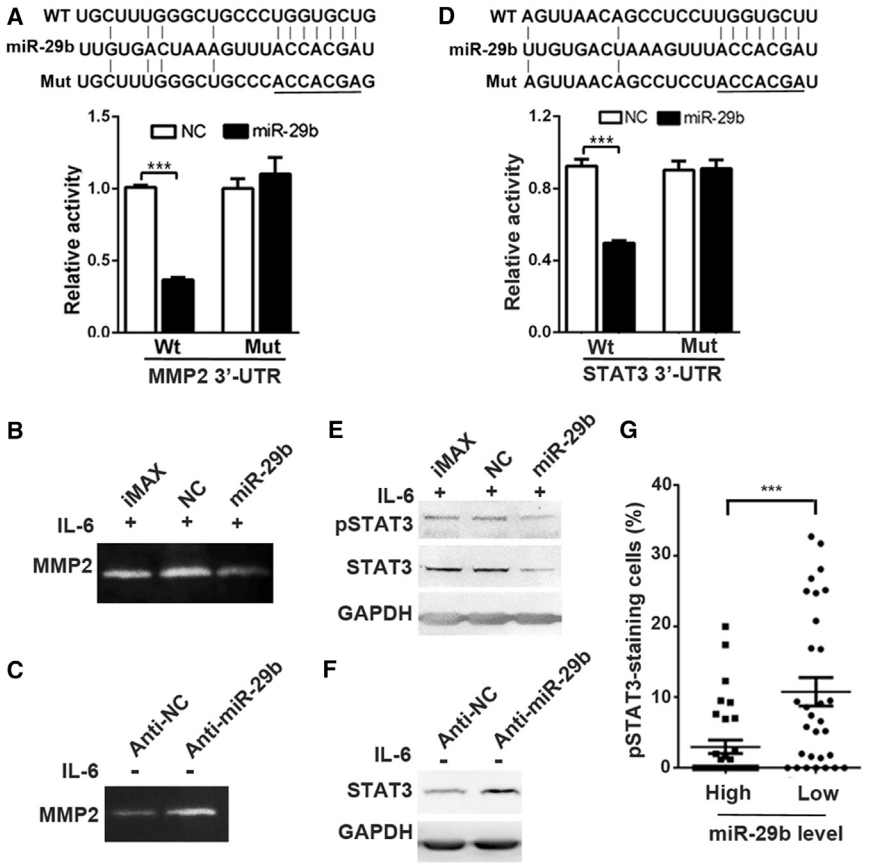

Figure 4. miR-29b Suppresses MMP2 and STAT3 Expression by Binding to Their 3′ UTR

(A) miR-29b suppressed gene expression by binding to the 3′ UTR of *MMP2* mRNA. Upper: miR-29b and its putative binding sequence in the 3′ UTR of *MMP2*. Lower: QGY-7703 cells were co-transfected with NC or miR-29b duplex, the luciferase reporter plasmid containing wild-type or mutant 3′ UTR of *MMP2* (indicated as Wt or Mut on the x axis), and a *Renilla* luciferase-expressing construct. (B and C) miR-29b inhibited the activity of MMP2. QGY-7703 cells were transfected with NC or miR-29b (B) or with anti-NC or anti-miR-29b (C) for 36 hr, followed by culture in serum-free DMEM with (+) or without (–) IL-6 for 24 hr. Conditioned medium from tumor cells (TCM) was then collected and applied to gelatin zymography analysis. (D) miR-29b suppressed gene expression by binding to the 3′ UTR of *STAT3* mRNA. Upper: miR-29b and its putative binding sequence in the 3′ UTR of *STAT3*. Lower: QGY-7703 cells were co-transfected with NC or miR-29b duplex, the luciferase reporter plasmid containing wild-type or mutant 3′ UTR of *STAT3* (indicated as Wt or Mut on the x axis), and a *Renilla* luciferase-expressing construct. (E and F) miR-29b reduced the cellular levels of STAT3 and its phosphorylated form. QGY-7703 cells were transfected with NC or miR-29b (E) or with anti-NC or anti-miR-29b (F) for 36 hr and then cultured in 5% FBS-containing DMEM with (+) or without (–) IL-6 for 0.5 hr before immunoblotting. For (B), (C), (E), and (F), iMAX indicates the cells that were transfected with Lipofectamine RNAiMAX without any duplex. NC and anti-NC indicate negative control for miR-29b and anti-miR-29b, respectively. GAPDH indicates internal control. (G) Human HCC tissues with lower miR-29b expression displayed a higher pSTAT3 level. The level of pSTAT3 was analyzed by immunohistochemical staining as in Figure 3G, and the level of miR-29b was detected by qPCR and normalized to RNU6. The median miR-29b level was chosen as the cutoff point to separate low-miR-29b-expressing tumors (n = 31) from high-miR-29b-expressing tumors (n = 32). Scale bar, 50 μm. Error bar, SEM. ***$p < 0.001$. See also Figures S5 and S6.

enhanced tube formation (Figure 5C), suggesting the suppressive role of miR-29b on VM formation in vitro. The anti-VM effect of miR-29b was verified in vivo. QGY-7703 cells were mixed with IL-6 and then implanted subcutaneously into the posterior flank of nude mice. The adeno-associated virus 8 (AAV8) that expressed miR-29b (AAV8-miR-29b) (Figure S7A) or GFP (AAV8-Ctrl) was then injected into either side of xenografts. Compared with the AAV8-Ctrl group, intratumoral injection of AAV8-miR-29b significantly inhibited VM formation (Figure 5D) and reduced microvessel density (MVD) (Figure S7B) and tumor growth (Figure S7C). Moreover, the level of miR-29b was lower in human VM^+ HCC tissues compared with VM^- ones (Figure 5E). Altogether, both in vitro and in vivo assays indicate the suppressive effect of miR-29b on VM formation.

We then verified whether miR-29b blocked VM formation by abrogating IL-6-STAT3 signaling. As shown, restoration of miR-29b expression dramatically attenuated the promoting effect of IL-6 on the expression of pSTAT3 and VE-Cad proteins and the activity of MMP2 (Figure 6A). Furthermore, overexpression of STAT3C, a constitutive active form of STAT3, antagonized the suppression of miR-29b on the VE-Cad expression and the tube formation of tumor cells (Figures 6B and 6C; Figure S8). Consistently, the AAV8-miR-29b-injected QGY-7703-xenografts (Figure 5D) displayed lower levels of pSTAT3 and MMP2 than the control ones (Figures 6D and 6E).

Collectively, these data indicate that miR-29b may inhibit the IL-6-stimulated VM formation by directly suppressing STAT3 and MMP2 expression and in turn repressing the IL-6-STAT3 signaling pathway (Figure 6F).

DISCUSSION

This work uncovers that IL-6, derived from tumor cells and stromal cells, activates STAT3 and, in turn, upregulates VE-Cad and MMP2 expression, and consequently promotes the VM formation of tumor cells. However, miR-29b significantly inhibits VM formation by directly suppressing STAT3 and MMP2 expression and in turn attenuating IL-6-STAT3 signaling transduction (Figure 6F). Our findings disclose a signaling cascade and an important mechanism

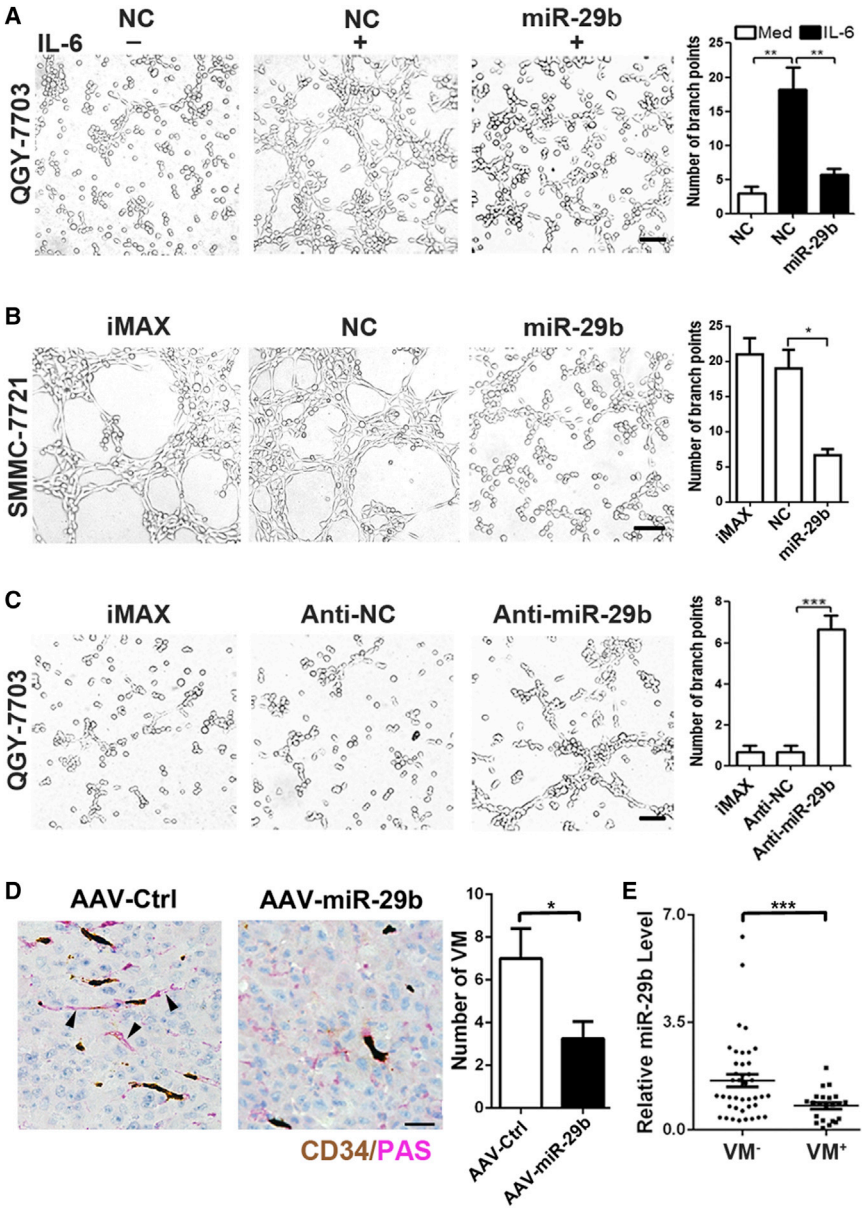

Figure 5. miR-29b Represses IL-6-Promoted VM Formation In Vitro and In Vivo

(A) Restoration of miR-29b expression significantly suppressed the IL-6-promoted tube formation of QGY-7703. Cells were transfected with NC (negative control) or miR-29b for 24 hr and then grown in 5% FBS-containing DMEM without (–) or with (+) IL-6 for another 24 hr before tube formation assay. (B) Restoration of miR-29b expression significantly suppressed the spontaneous tube formation of SMMC-7721 cells. Cells were transfected with NC or miR-29b for 36 hr before tube formation assay. (C) Antagonism of cellular endogenous miR-29b enhanced the tube formation of QGY-7703 cells. Cells were transfected with anti-NC (negative control) or anti-miR-29b for 48 hr before tube formation assay. For (A)–(C), iMAX indicates the cells that were transfected with Lipofectamine RNAiMAX without any duplex. (D) miR-29b inhibited the IL-6-promoted VM formation in vivo. QGY-7703 cells (1×10^6) mixed with IL-6 (200 ng) were implanted into nude mice subcutaneously. AAV8-Ctrl or AAV8-miR-29b were intratumorally injected at the 5th day and 9th day post-implantation (n = 8 for each group). Tumors were dissected 5 days after the last injection of viruses and applied to analyses for VM formation. The vascular channels that were lined by tumor cells, but not endothelial cells (PAS^+CD34^-), were designated as VM structures (indicated by arrowheads). The endothelial vessels were stained brown by antibody against mCD34. (E) The miR-29b level was significant lower in human VM^+ HCC tissues. The level of miR-29b in VM^- tissues (n = 41) and VM^+ tissues (n = 22) was detected by qPCR, and RNU6 was used as an internal control, as in Figure 4G. Scale bar, 50 μm. Error bar, SEM.*p < 0.05; **p < 0.01; ***p < 0.001. See also Figure S7.

of VM formation, which provides potential targets for anti-cancer therapy.

The tumor microcirculation plays a central role in the rapid growth and hematogenous dissemination of cancer cells.[26,27] Endothelium-dependent vessels, which require the recruitment of normal endothelial cells, may not be sufficient to sustain aggressive tumor growth at the early stage of rapid growth. It is proposed that VM and mosaic vessels are the major sources of blood supply at early stage of tumor formation.[14,17,20,28,29] Another interesting observation is that VM is most frequently observed in the boundary region between tumor and adjacent normal tissue, where tumor cells are rapidly growing.[17,28,29] Studies in the xenografts reveal the existence of blood perfusion between the endothelial-lined vasculature and the VM networks,[28,29] and the presence of VM was associated with both shorter recurrence-free survival and overall survival of patients.[9,10,18,19] Collectively, VM is an important complement of tumor microcirculation, and it provides an alternative pathway for tumor growth and metastasis. However, the underlying mechanism of VM formation remains unclear. Studies have reported that PI3K/Akt signaling participates in VM formation by regulating the activity of MMP2.[9,10] PI3K/Akt increases MT1-MMP activity, resulting in transition of pro-MMP2 into active MMP2. Then, MMP2 cleaves the laminin (Ln) 5γ2 chain into γ2 and γ2*x* fragments, which are deposited in the ECM and induce VM formation. VE-Cad also plays a significant role in VM formation by increasing the level of phosphorylated EphA2.[9,10] The phosphorylated EphA2 activates PI3K and FAK, which both lead to MMP2 activation and subsequent Ln-5γ2 cleavage. Here, we demonstrated that IL-6 signaling is an important regulatory mechanism of VM formation based on in vitro and in vivo analyses. First, recombinant IL-6 protein or tumor cell- and stromal cell-secreted IL-6 was able to promote tumor cells to

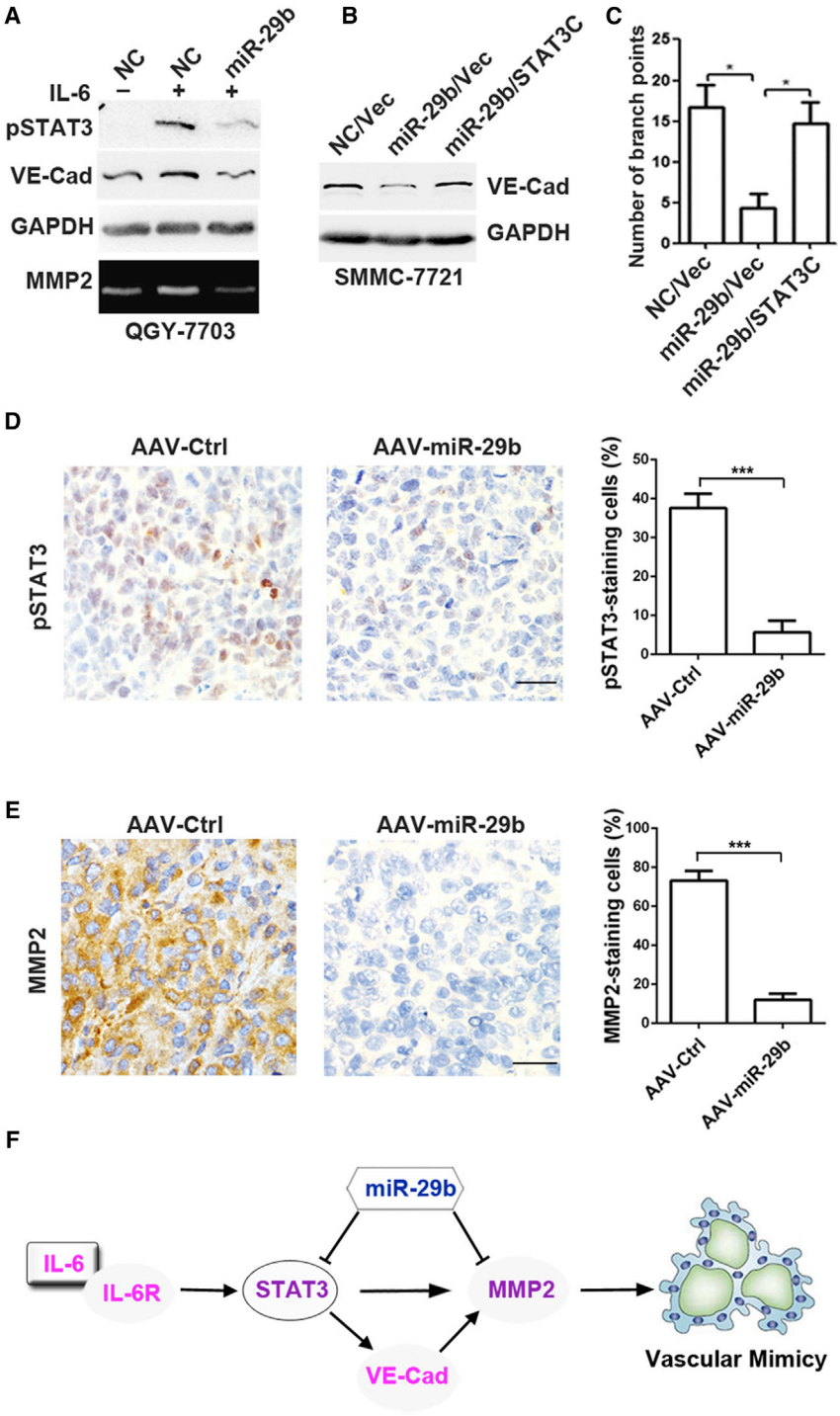

Figure 6. miR-29b Blocks IL-6-Promoted VM Formation by Abrogating IL-6-STAT3-VE-Cad-MMP2 Signaling

(A) miR-29b attenuated IL-6-promoted VE-Cad expression and MMP2 activity. For immunoblotting, QGY-7703 cells that were transfected with NC or miR-29b were cultured in serum-free DMEM for 24 hr, followed by incubation with the refreshed serum-free DMEM without (–) or with (+) IL-6 for 2 hr. For gelatin zymography analysis, QGY-7703 cells that were transfected with NC or miR-29b were cultured in serum-free DMEM without or with IL-6 for 24 hr. (B and C) Activated STAT3 abolished the suppressive effect of miR-29b on VE-Cad expression and tube formation. SMMC-7721 cells were co-transfected with the indicated plasmid (200 ng) and RNA duplex (50 nM) for 48 hr and then applied to immunoblotting (B) or tube formation assay (C). Vec indicates the pcDNA3-EGFP vector expressing EGFP only. STAT3C indicates the pcDNA3-EGFP-STAT3C vector expressing both EGFP and constitutively activated STAT3 under the control of different promoters. GAPDH indicates the internal control. (D and E) The AAV8-miR-29b-infected xenografts displayed lower levels of pSTAT3 and MMP2. The percentages of pSTAT3-staining cells (D) and MMP2-staining cells (E) in the QGY-7703-xenografts (n = 8 for each group) were analyzed by immunohistochemical staining. Scale bar, 50 μm. (C–E) Error bar, SEM. *p < 0.05; ***p < 0.001. (F) The paradigm of the miR-29b-IL-6 signaling in VM formation. See also Figure S8.

form capillary-like tubes in vitro. Blocking IL-6 signal transduction either by knocking down the expression of IL-6, IL-6R, or STAT3, or by IL-6-neutralizing antibody or STAT3 inhibitor, abolished the IL-6-promoted tube formation of tumor cells. Second, both gain- and lost-of-function studies disclosed that IL-6 activated STAT3 and, in turn, upregulated VE-Cad and MMP2 expression, and consequently resulted in VM formation. Third, analysis on clinical samples revealed that the activation of IL-6-STAT3 signaling was positively correlated with the number of VM structures in HCC tissues.

Previous studies on VM have focused on the tumor cell, such as tumor plasticity, and ECM remodeling.[9,12–15] However, the effect of the tumor microenvironment on VM formation was less explored. CAFs and TAMs are the major constituents of the microenvironment that contributes to tumor progression.[4,5,26,27] The roles of CAFs and TAMs in VM formation remain unclear. Recently, we showed that the CAF-secreted transforming growth factor β (TGF-β) and SDF1 enhanced the expression of VE-cad, MMP2, and Ln-5γ2 via TGF-βR1 and CXCR4 in tumor cells, thereby promoted VM formation.[30] At the same time, a study from another group showed that the conditioned medium derived from the M2 macrophage promoted tube formation of glioma cells in vitro by amplifying IL-6 expression in glioma cells.[31] However, this study only conducted an in vitro tube formation assay and did not explored how IL-6 exerted the tube formation-promoting function. So far, these are the only two reports to show the roles of fibroblasts and macrophages in VM formation. Our study further

highlights the significance of CAFs and TAMs in VM formation and discloses the underlying mechanisms. Here we showed that compared with CM-NF or CM from macrophages, CM-CAF and CM-TAM displayed a much higher level of IL-6 and a much stronger capability to enhance STAT3 phosphorylation and VM formation of tumor cells. CM-CAF- and CM-TAM-promoted STAT3 phosphorylation and VM formation were significantly attenuated when IL-6-neutralizing antibody or STAT3 inhibitor was added or when IL-6R or STAT3 expression in tumor cells was silenced. These data indicate that CAFs and TAMs may promote VM formation by secreting IL-6, resulting in activation of IL-6-STAT3 signaling in tumor cells.

Traditional anti-angiogenesis drugs, such as anginex and endostatin, have been shown to be ineffective in inhibiting VM.[18–20] Identification of potential targets, which can be applied to inhibit both angiogenesis and VM formation, may be effective in abolishing tumor microcirculation and tumor progression. miRNAs are attractive targets for cancer therapy, because they may regulate cellular activity by targeting multiple genes.[25] miR-29b is frequently downregulated in different types of cancers, and it can promote cell apoptosis and inhibit proliferation, tumor angiogenesis, and metastasis. It was reported that miR-29b overexpression inhibited the activity of a luciferase reporter containing STAT3 3′ UTR and decreased the level of STAT3 mRNA and protein in HER2-positive breast cancer cells.[32] However, the relation of miR-29b and STAT3 in vivo and whether miR-29b affects IL-6-induced STAT3 activation and VM formation have not been explored yet. In this study, based on human HCC specimens and cell and animal models, we showed that miR-29b significantly suppressed the IL-6-promoted VM formation of tumor cells by targeting STAT3 and in turn blocking IL-6 signaling transduction. MMP2, which could be transcriptionally induced by STAT3 and played a vital role in VM formation,[8,9] was also a direct target of miR-29b in this model. Considering its role in promoting apoptosis and suppressing proliferation, VM formation, angiogenesis, and metastasis, miR-29b should represent a promising molecule for anti-cancer therapy.

In summary, we disclose the importance of tumor stromal cells and miR-29b-IL-6-STAT3 signaling in the VM formation of HCC cells. These findings should be applicable to other types of tumors, because IL-6 activation and miR-29b downregulation are prevalent events in tumor cells and are associated with excessive growth, invasion, and angiogenesis of different types of cancers.

MATERIALS AND METHODS

More details are provided in Supplemental Materials and Methods.

Human Tissue Specimens

All tissues were obtained from pathologically confirmed HCC patients who underwent HCC resection at the Cancer Center, Sun Yat-sen University. No local or systemic treatment had been conducted before operation. Informed consent was obtained from each patient, and the protocol was approved by the Institutional Research Ethics Committee, Sun Yat-sen University. The patients were anonymously coded in accordance with ethical guidelines, as instructed by the Declaration of Helsinki.

Reagents

The antibodies and chemicals used were as follows: mouse monoclonal antibodies (mAbs) against Tyr705-pSTAT3 (sc-8059, Santa Cruz Biotechnology), STAT3 (sc-8019, Santa Cruz Biotechnology), GAPDH (BM1623, Boster), human cell surface glycoprotein CD34 (hCD34, clone QBEnd/10, Santa Cruz Biotechnology), rat mAb against mouse CD34 (mCD34, clone MEC14.7, BioLegend), and rabbit polyclonal antibody (pAb) against VE-Cad (ab33168, Abcam). Recombinant human IL-6 protein (206-IL-050, R&D Systems) was dissolved at 100 μg/mL in serum-free DMEM (Life Technologies) and was used at a final concentration of 50 ng/mL. Neutralizing antibody against IL-6 (anti-IL-6, No. 6708, R&D Systems) was used at a final concentration of 40 μg/mL. The inhibitor of STAT3, S3I-201 (S1155, Selleck Chemicals), was dissolved at 100 mM in DMSO (Sigma-Aldrich) and was used at a final concentration of 100 μM.

Tumor Cell Lines

The human HCC cell lines, including QGY-7703 and SMMC-7721, were maintained in DMEM supplemented with 10% fetal bovine serum (FBS, Hyclone).

Isolation and Culture of CAFs and NFs

Fresh HCC specimens and the matched non-tumor liver tissues were collected to isolate CAFs and NFs, respectively. Tissues were rinsed in 1× PBS containing penicillin (100 U/mL) and streptomycin (0.1 mg/mL) and then sliced into small pieces (~8 mm^3). The necrotic tissues were carefully removed. The sliced tissue was incubated at 37°C for 2–6 hr in DMEM containing digestion enzymes (100 U/mL hyaluronidase, Life Technologies; 1 mg/mL collagenase type I, Sigma-Aldrich), with periodic shaking. Afterward, the tissue lysate was diluted in 1× PBS and centrifuged at 400 × *g* for 8 min. The cell pellet was then collected and re-suspended in 40 mL fresh 1× PBS. The centrifugation and re-suspension steps were repeated three times, followed by seeding the cells at a concentration of 1×10^6 cells/mL in RPMI-1640 (RPMI, Life Technologies) supplemented with 10% FBS, penicillin (100 U/mL), and streptomycin (0.1 mg/mL). Two primary NFs and CAFs were successfully isolated from two HCC patients (patients 1 and 2). Unless otherwise indicated, the patient 1 CAF was employed for the analysis.

Establishment of Macrophages and TAMs

Ficoll (GE Healthcare Life Sciences) density gradient centrifugation was used to isolate human peripheral blood mononuclear cells (PBMCs) from leukocyte-enriched buffy coats obtained from healthy donors. Monocytes were further isolated from PBMCs by CD14-positive selection using magnetic-activated cell sorting (MACS) technology (Miltenyi Biotec) and then cultured for 2–3 days in DMEM supplemented with 10% human AB serum to differentiate into macrophages or further followed by incubation with 15% CM of QGY-7703 cells for 6 days to generate TAMs. Two primary macrophages and their corresponding TAMs were established from two healthy

donors (donors 3 and 4). Unless otherwise indicated, the donor 3 TAM was employed for the analysis.

The CM of tumor cells used for TAM establishment was prepared as follows: QGY-7703 cells (5×10^6) were plated in a 100-mm dish containing 10 mL DMEM with 10% FBS for 24 hr, followed by refreshment with DMEM supplemented with 10% human AB serum and incubation for another 48 hr. The CM was collected and centrifuged at $500 \times g$ to remove detached cells and then at $12{,}000 \times g$ to discard cell debris (4°C, 10 min for each). The aliquots were stored at −80°C until use.

Preparation of CM-NF, CM-CAF, and CM from Macrophages and CM-TAM

NFs, CAFs, macrophages, or TAMs (1×10^5) were plated in a 12-well dish for 24 hr, followed by refreshment with 500 μL DMEM supplemented with 10% FBS and further incubation for 24 hr. The CM was collected and centrifuged at $500 \times g$ to remove detached cells and then at $12{,}000 \times g$ to discard cell debris (4°C, 10 min for each). The aliquots were stored at −80°C until use.

Three-Dimensional Tube Formation Assays

Tumor cells with different treatments were digested, counted, and re-suspended in 5% FBS-containing DMEM and then applied to tube formation assay, which was performed by seeding 3.5×10^4 tumor cells (in 200 μL, 5% FBS-containing DMEM) in a 48-well plate pre-coated with Matrigel (at a concentration of 60%, 3432-005-01, R&D Systems) and then incubated for 6 hr. The formation of capillary-like structures was captured under a light microscope. The branch points of the formed tubes, which represented the degree of VM in vitro, were scanned and quantitated in five fields (200×).

To avoid the bias induced by distinct growth rates of cells that underwent different treatments, tumor cells with various treatments were digested, counted, and re-suspended in the same density and incubated on Matrigel for 6 hr. The total numbers of cells with or without exposure to IL-6, STAT3 inhibitor, or IL-6 neutralizing antibody were similar at the end of tube formation assay.

RNA Oligoribonucleotides, Vectors, and AAV8

Small interfering RNA (siRNA) duplexes, miR-29b mimics, and miR-29b inhibitor (anti-miR-29b) were purchased from GenePharma. The firefly luciferase reporter system was used to verify the 3′ UTR that were targeted by miR-29b. To create luciferase reporter construct, a wild-type or mutant 3′ UTR segment of target mRNA was inserted downstream of the stop codon of firefly luciferase in the pGL3cm vector,[33] a modified pGL3-control vector (Promega). The pcDNA3-EGFP-STAT3C vector was used to express EGFP and constitutively active STAT3. AAV8 system was used to deliver miR-29b in vivo.

All constructs were verified by direct DNA sequencing. The sequences of RNA oligoribonucleotides and primers are provided in Table S1.

Cell Transfections

Reverse transfection of RNA oligoribonucleotides and co-transfection of RNA duplex with plasmid DNA were performed using Lipofectamine RNAiMAX and Lipofectamine 2000 (Life Technologies), respectively.

Mouse Xenograft Models

All procedures for animal experiments were performed in accordance with the Guide for the Care and Use of Laboratory Animals (NIH publication No. 80-23, revised 1996) and according to the Sun Yat-sen University Institutional Ethical Guidelines for animal experiments.

To analyze the effect of miR-29b on the IL-6-promoted VM formation in vivo, QGY-7703 cells (1×10^6) mixed with IL-6 (200 ng) were injected subcutaneously into both sides of the posterior flank of BALB/c nude mice at 4 weeks of age. AAV8-miR-29b or AAV8-Ctrl (1×10^{11} vector genomes) were injected into xenografts at the 5^{th} day and 9^{th} day post-implantation, and tumors were dissected 5 days after the last injection of viruses, fixed in 10% formalin, and embedded in paraffin.

The length (L) and width (W) of the dissected tumors were measured, and the tumor volume (V) was calculated using the formula $V = (L \times W^2) \times 0.5$.

IHC and PAS Staining

Paraffin-embedded tissue sections were applied to immunohistochemistry (IHC). To investigate VM structure, tissues, which were stained with CD34, were further counterstained by PAS (cat. BA4080A, BASO) and hematoxylin.

pSTAT3 and MMP2 expression was evaluated under a light microscope at a magnification of 400×. For each sample, a total of 1,000 to ∼2,000 tumor cells were analyzed. The percentage of the pSTAT3- or MMP2-staining cells was calculated.

The MVD, which represents the degree of angiogenesis in vivo, was evaluated by staining for mCD34 in xenografts. Any stained discrete cluster or single cell was counted as one microvessel, and the average number of microvessels per field (200×) was presented as MVD.

Luciferase Reporter Assay

QGY-7703 cells and SMMC-7721 cells in a 48-well plate were co-transfected with RNA duplex and luciferase reporter plasmid and then applied to luciferase assay as described.[33]

Analysis of Gene Expression

Gene level was analyzed by real-time qPCR, western blotting, or ELISA.

Gelatin Zymography

The activity of MMP2 in the CM of tumor cells was detected by gelatin zymography.

Immunofluorescent Staining

SMMC-7721 cells were applied to immunofluorescent staining using primary antibody against pSTAT3.

Statistical Analysis

Data are expressed as the mean ± SEM. Unless otherwise indicated, for all in vitro experiments, data from three independent experiments were analyzed. For mouse and clinical samples, the numbers of mice or patients were indicated in the corresponding figure legends. The differences between groups were analyzed using Student's t test when only two groups were compared or by one-way ANOVA when more than two groups were compared. All statistical tests were two sided. Differences were considered statistically significant at $p < 0.05$. All analyses were performed with GraphPad Prism v.5 (GraphPad).

SUPPLEMENTAL INFORMATION

Supplemental Information includes Supplemental Materials and Methods, eight figures, and one table and can be found with this article online at http://dx.doi.org/10.1016/j.omtn.2017.06.009.

AUTHOR CONTRIBUTIONS

J.-H.F., Z.-Y.Z., and S.-M.Z. designed the study. J.-H.F., Z.-Y.Z., J.-Y.L., C.X., and Z.-J.Z. conducted the experiments. J.-H.F., Z.-Y.Z., and S.-M.Z. analyzed and interpreted the data and wrote the paper. All authors read and approved the final manuscript. J.-H.F. and S.-M.Z. provided funding for the study.

CONFLICTS OF INTEREST

No potential conflicts of interest were disclosed.

ACKNOWLEDGMENTS

This work was supported by grants from National Natural Science Foundation of China (81230049, 81401922, and 91440205), Natural Science Foundation of Guangdong Province (2014A030311031), Science and Information Technology of Guangzhou (201610010056), and Fundamental Research Funds for the Central Universities (16lgpy29 and 16lgjc42).

REFERENCES

1. Hunter, C.A., and Jones, S.A. (2015). IL-6 as a keystone cytokine in health and disease. Nat. Immunol. *16*, 448–457.
2. Rossi, J.F., Lu, Z.Y., Jourdan, M., and Klein, B. (2015). Interleukin-6 as a therapeutic target. Clin. Cancer Res. *21*, 1248–1257.
3. Mauer, J., Denson, J.L., and Bruning, J.C. (2015). Versatile functions for IL-6 in metabolism and cancer. Trends Immunol. *36*, 92–101.
4. Wan, S., Zhao, E., Kryczek, I., Vatan, L., Sadovskaya, A., Ludema, G., Simeone, D.M., Zou, W., and Welling, T.H. (2014). Tumor-associated macrophages produce interleukin 6 and signal via STAT3 to promote expansion of human hepatocellular carcinoma stem cells. Gastroenterology *147*, 1393–1404.
5. Li, P., Shan, J.X., Chen, X.H., Zhang, D., Su, L.P., Huang, X.Y., Yu, B.Q., Zhi, Q.M., Li, C.L., Wang, Y.Q., et al. (2015). Epigenetic silencing of microRNA-149 in cancer-associated fibroblasts mediates prostaglandin E2/interleukin-6 signaling in the tumor microenvironment. Cell Res. *25*, 588–603.
6. Shinriki, S., Jono, H., Ueda, M., Ota, K., Ota, T., Sueyoshi, T., Oike, Y., Ibusuki, M., Hiraki, A., Nakayama, H., et al. (2011). Interleukin-6 signalling regulates vascular endothelial growth factor-C synthesis and lymphangiogenesis in human oral squamous cell carcinoma. J. Pathol. *225*, 142–150.
7. He, G., Dhar, D., Nakagawa, H., Font-Burgada, J., Ogata, H., Jiang, Y., Shalapour, S., Seki, E., Yost, S.E., Jepsen, K., et al. (2013). Identification of liver cancer progenitors whose malignant progression depends on autocrine IL-6 signaling. Cell *155*, 384–396.
8. Yu, H., Lee, H., Herrmann, A., Buettner, R., and Jove, R. (2014). Revisiting STAT3 signalling in cancer: new and unexpected biological functions. Nat. Rev. Cancer *14*, 736–746.
9. Seftor, R.E., Hess, A.R., Seftor, E.A., Kirschmann, D.A., Hardy, K.M., Margaryan, N.V., and Hendrix, M.J. (2012). Tumor cell vasculogenic mimicry: from controversy to therapeutic promise. Am. J. Pathol. *181*, 1115–1125.
10. Kirschmann, D.A., Seftor, E.A., Hardy, K.M., Seftor, R.E., and Hendrix, M.J. (2012). Molecular pathways: vasculogenic mimicry in tumor cells: diagnostic and therapeutic implications. Clin. Cancer Res. *18*, 2726–2732.
11. Cao, Z., Bao, M., Miele, L., Sarkar, F.H., Wang, Z., and Zhou, Q. (2013). Tumour vasculogenic mimicry is associated with poor prognosis of human cancer patients: a systemic review and meta-analysis. Eur. J. Cancer *49*, 3914–3923.
12. Sun, T., Sun, B.C., Zhao, X.L., Zhao, N., Dong, X.Y., Che, N., Yao, Z., Ma, Y.M., Gu, Q., Zong, W.K., and Liu, Z.Y. (2011). Promotion of tumor cell metastasis and vasculogenic mimicry by way of transcription coactivation by Bcl-2 and Twist1: a study of hepatocellular carcinoma. Hepatology *54*, 1690–1706.
13. Sun, T., Zhao, N., Zhao, X.L., Gu, Q., Zhang, S.W., Che, N., Wang, X.H., Du, J., Liu, Y.X., and Sun, B.C. (2010). Expression and functional significance of Twist1 in hepatocellular carcinoma: its role in vasculogenic mimicry. Hepatology *51*, 545–556.
14. Maniotis, A.J., Folberg, R., Hess, A., Seftor, E.A., Gardner, L.M., Pe'er, J., Trent, J.M., Meltzer, P.S., and Hendrix, M.J. (1999). Vascular channel formation by human melanoma cells in vivo and in vitro: vasculogenic mimicry. Am. J. Pathol. *155*, 739–752.
15. Wagenblast, E., Soto, M., Gutierrez-Angel, S., Hartl, C.A., Gable, A.L., Maceli, A.R., Erard, N., Williams, A.M., Kim, S.Y., Dickopf, S., et al. (2015). A model of breast cancer heterogeneity reveals vascular mimicry as a driver of metastasis. Nature *520*, 358–362.
16. Weis, S.M., and Cheresh, D.A. (2011). Tumor angiogenesis: molecular pathways and therapeutic targets. Nat. Med. *17*, 1359–1370.
17. Zhang, S., Guo, H., Zhang, D., Zhang, W., Zhao, X., Ren, Z., and Sun, B. (2006). Microcirculation patterns in different stages of melanoma growth. Oncol. Rep. *15*, 15–20.
18. Schnegg, C.I., Yang, M.H., Ghosh, S.K., and Hsu, M.Y. (2015). Induction of vasculogenic mimicry overrides VEGF-A silencing and enriches stem-like cancer cells in melanoma. Cancer Res. *75*, 1682–1690.
19. Xu, Y., Li, Q., Li, X.Y., Yang, Q.Y., Xu, W.W., and Liu, G.L. (2012). Short-term anti-vascular endothelial growth factor treatment elicits vasculogenic mimicry formation of tumors to accelerate metastasis. J. Exp. Clin. Cancer Res. *31*, 16.
20. van der Schaft, D.W., Seftor, R.E., Seftor, E.A., Hess, A.R., Gruman, L.M., Kirschmann, D.A., Yokoyama, Y., Griffioen, A.W., and Hendrix, M.J. (2004). Effects of angiogenesis inhibitors on vascular network formation by human endothelial and melanoma cells. J. Natl. Cancer Inst. *96*, 1473–1477.
21. Fang, J.H., Zhou, H.C., Zeng, C., Yang, J., Liu, Y., Huang, X., Zhang, J.P., Guan, X.Y., and Zhuang, S.M. (2011). MicroRNA-29b suppresses tumor angiogenesis, invasion, and metastasis by regulating matrix metalloproteinase 2 expression. Hepatology *54*, 1729–1740.
22. Xiong, Y., Fang, J.H., Yun, J.P., Yang, J., Zhang, Y., Jia, W.H., and Zhuang, S.M. (2010). Effects of microRNA-29 on apoptosis, tumorigenicity, and prognosis of hepatocellular carcinoma. Hepatology *51*, 836–845.
23. Zhao, J.J., Lin, J., Lwin, T., Yang, H., Guo, J., Kong, W., Dessureault, S., Moscinski, L.C., Rezania, D., Dalton, W.S., et al. (2010). microRNA expression profile and identification of miR-29 as a prognostic marker and pathogenetic factor by targeting CDK6 in mantle cell lymphoma. Blood *115*, 2630–2639.
24. Jonas, S., and Izaurralde, E. (2015). Towards a molecular understanding of microRNA-mediated gene silencing. Nat. Rev. Genet. *16*, 421–433.
25. Li, Z., and Rana, T.M. (2014). Therapeutic targeting of microRNAs: current status and future challenges. Nat. Rev. Drug Discov. *13*, 622–638.

26. Friedl, P., and Alexander, S. (2011). Cancer invasion and the microenvironment: plasticity and reciprocity. Cell *147*, 992–1009.

27. Turley, S.J., Cremasco, V., and Astarita, J.L. (2015). Immunological hallmarks of stromal cells in the tumour microenvironment. Nat. Rev. Immunol. *15*, 669–682.

28. Ruf, W., Seftor, E.A., Petrovan, R.J., Weiss, R.M., Gruman, L.M., Margaryan, N.V., Seftor, R.E., Miyagi, Y., and Hendrix, M.J. (2003). Differential role of tissue factor pathway inhibitors 1 and 2 in melanoma vasculogenic mimicry. Cancer Res. *63*, 5381–5389.

29. Shirakawa, K., Kobayashi, H., Heike, Y., Kawamoto, S., Brechbiel, M.W., Kasumi, F., Iwanaga, T., Konishi, F., Terada, M., and Wakasugi, H. (2002). Hemodynamics in vasculogenic mimicry and angiogenesis of inflammatory breast cancer xenograft. Cancer Res. *62*, 560–566.

30. Yang, J., Lu, Y., Lin, Y.Y., Zheng, Z.Y., Fang, J.H., He, S., and Zhuang, S.M. (2016). Vascular mimicry formation is promoted by paracrine TGF-β and SDF1 of cancer-associated fibroblasts and inhibited by miR-101 in hepatocellular carcinoma. Cancer Lett. *383*, 18–27.

31. Zhang, L., Xu, Y., Sun, J., Chen, W., Zhao, L., Ma, C., Wang, Q., Sun, J., Huang, B., Zhang, Y., et al. (2017). M2-like tumor-associated macrophages drive vasculogenic mimicry through amplification of IL-6 expression in glioma cells. Oncotarget *8*, 819–832.

32. Qin, L., Li, R., Zhang, J., Li, A., and Luo, R. (2015). Special suppressive role of miR-29b in HER2-positive breast cancer cells by targeting Stat3. Am. J. Transl. Res. *7*, 878–890.

33. Su, H., Yang, J.R., Xu, T., Huang, J., Xu, L., Yuan, Y., and Zhuang, S.M. (2009). MicroRNA-101, down-regulated in hepatocellular carcinoma, promotes apoptosis and suppresses tumorigenicity. Cancer Res. *69*, 1135–1142.